INTERNATIONAL JOURNAL FOR NUMERICAL METHODS IN ENGINEERING
Int. J. Numer. Meth. Engng 2008; **76**:2091–2116
Published online 10 July 2008 in Wiley InterScience (www.interscience.wiley.com). DOI: 10.1002/nme.2394

A polynomial dimensional decomposition for stochastic computing

Sharif Rahman*, †, ‡

Department of Mechanical and Industrial Engineering, College of Engineering, The University of Iowa, Iowa City, IA 52242, U.S.A.

SUMMARY

This article presents a new polynomial dimensional decomposition method for solving stochastic problems commonly encountered in engineering disciplines and applied sciences. The method involves a hierarchical decomposition of a multivariate response function in terms of variables with increasing dimensions, a broad range of orthonormal polynomial bases consistent with the probability measure for Fourier-polynomial expansion of component functions, and an innovative dimension-reduction integration for calculating the coefficients of the expansion. The new decomposition method does not require sample points as in the previous version; yet, it generates a convergent sequence of lower-variate estimates of the probabilistic characteristics of a generic stochastic response. The results of five numerical examples indicate that the proposed decomposition method provides accurate, convergent, and computationally efficient estimates of the tail probability of random mathematical functions or the reliability of mechanical systems. Copyright © 2008 John Wiley & Sons, Ltd.

Received 23 November 2007; Revised 6 May 2008; Accepted 7 May 2008

KEY WORDS: uncertainty analysis; probabilistic mechanics; reliability; orthogonal polynomials; Fourier-polynomial expansion; ANOVA; polynomial chaos; Monte Carlo simulation

1. INTRODUCTION

A wide variety of stochastic methods, comprising simulation, numerical integration, and analytical methods, exist in the current literature for calculating the probabilistic characteristics of response of stochastic systems [1, 2]. Although simulation methods can solve any stochastic problem, they generally require a large number of deterministic trials to calculate low probability and are prohibitive when each trial involves expensive numerical calculation. The analytical methods

*Correspondence to: Sharif Rahman, Department of Mechanical and Industrial Engineering, College of Engineering, The University of Iowa, Iowa City, IA 52242, U.S.A.
†E-mail: rahman@engineering.uiowa.edu
‡Professor.

Contract/grant sponsor: U.S. National Science Foundation; contract/grant numbers: DMI-0355487, CMMI-0653279

require additional assumptions, mostly for computational expediency, that begin to break down when the input–output mapping is highly non-linear and the input uncertainty is large. More importantly, many high-dimensional problems are all but impossible to solve using analytical methods or numerical integration. The root deterrence to practical computability is often related to the high dimension of the multivariate integration or interpolation problem, known as the curse of dimensionality [3]. The curse of dimensionality means that the computational cost increases exponentially with the dimension of the problem. The recently developed dimensional decomposition [4, 5] of a multivariate function addresses the curse of dimensionality by developing an input–output behavior of complex stochastic systems with low effective dimension [6], where the degree of cooperativity between variables dies off rapidly.

Past stochastic studies stemming from the dimensional decomposition require a reference point, commonly assumed to be the mean value of the random input and sample points surrounding that reference point [5]. Based on these sample points, deterministic calculations of a performance function, either exactly or numerically, are conducted to generate Lagrange interpolations of various component functions embedded in the decomposition. They lead to a hierarchical sequence of approximations of a stochastic response, each described by an explicit function of the random input. There are two weaknesses in this procedure. First, the decomposition constructed above depends on a selected reference point. It is elementary to show that an improper or careless selection of the reference point can spoil the approximation. Second and more importantly, the sample points are vaguely selected with no strict guidelines. For instance, sample points are commonly deployed based on the standard deviation of the random input, but still it is an arbitrary decision [5]. If an input variable is strictly positive (or strictly negative) or follows a probability density with compact support, the resultant sample points from the current practice may fall outside the physical domain. In that case, existing decomposition methods may either fail or generate unrealistic sample properties of a random output. Therefore, alternative means of approximating the component functions by dropping the sample points altogether are highly desirable.

This paper presents a new polynomial dimensional decomposition method for solving stochastic problems encountered in engineering and science disciplines. The method is based on (1) a hierarchical decomposition of a multivariate response function in terms of variables with increasing dimensions, (2) a broad range of orthonormal polynomial bases consistent with the probability measure for Fourier-polynomial expansion of component functions, and (3) an innovative dimension-reduction integration for calculating the coefficients of the expansion. Section 2 reviews a generic dimensional decomposition and its various component functions. Section 3 presents orthonormal polynomials in developing the Fourier-polynomial expansion of the component functions. The formulation of the coefficients of the expansion and their numerical evaluation by the dimension-reduction integration are described. The section also discusses the computational flow and required effort. Section 4 compares the polynomial dimensional decomposition with the existing polynomial chaos expansion. Five numerical examples illustrate the accuracy, convergence, and computational efficiency of the proposed method in Section 5. Conclusions are drawn in Section 6.

2. MULTIVARIATE FUNCTION DECOMPOSITION

Consider a continuous, differentiable, real-valued, multivariate function $y(\mathbf{x})$ that depends on $\mathbf{x} = \{x_1, \ldots, x_N\}^{\mathrm{T}} \in \mathbb{R}^N$, where $\mathbb{R}^N$ is an N-dimensional real vector space. A dimensional decomposition

DOI: 10.1002/nme

of $y(\mathbf{x})$, described by [4, 5, 7–11]

$$y(\mathbf{x}) = y_0 + \sum_{i=1}^{N} y_i(x_i) + \sum_{i_1,i_2=1;i_1<i_2}^{N} y_{i_1 i_2}(x_{i_1}, x_{i_2}) + \sum_{i_1,i_2,i_3=1;i_1<i_2<i_3}^{N} y_{i_1 i_2 i_3}(x_{i_1}, x_{i_2}, x_{i_3})$$
$$+ \cdots + \sum_{i_1,\ldots,i_S=1;i_1<\cdots<i_S}^{N} y_{i_1\cdots i_S}(x_{i_1}, \ldots, x_{i_S}) + \cdots + y_{12\cdots N}(x_1, \ldots, x_N) \tag{1}$$

can be viewed as a finite hierarchical expansion of an output function in terms of its input variables with increasing dimensions, where y_0 is a constant, $y_i(x_i)$ is a univariate component function representing individual contribution to $y(\mathbf{x})$ by input variable x_i acting alone, $y_{i_1 i_2}(x_{i_1}, x_{i_2})$ is a bivariate component function describing the cooperative influence of two input variables x_{i_1} and x_{i_2}, $y_{i_1 i_2 i_3}(x_{i_1}, x_{i_2}, x_{i_3})$ is a trivariate component function describing the cooperative influence of three input variables x_{i_1}, x_{i_2}, and x_{i_3}, $y_{i_1\cdots i_S}(x_{i_1}, \ldots, x_{i_S})$ is an S-variate component function quantifying the cooperative effects of S input variables $x_{i_1}, \ldots, x_{i_S}$, and so on. The last term in Equation (1) represents any residual dependence of all input variables cooperatively locked together to affect the output function y. If

$$\tilde{y}_S(\mathbf{x}) = y_0 + \sum_{i=1}^{N} y_i(x_i) + \sum_{i_1,i_2=1;i_1<i_2}^{N} y_{i_1 i_2}(x_{i_1}, x_{i_2}) + \sum_{i_1,i_2,i_3=1;i_1<i_2<i_3}^{N} y_{i_1 i_2 i_3}(x_{i_1}, x_{i_2}, x_{i_3})$$
$$+ \cdots + \sum_{i_1,\ldots,i_S=1;i_1<\cdots<i_S}^{N} y_{i_1\cdots i_S}(x_{i_1}, \ldots, x_{i_S}) \tag{2}$$

represents a general S-variate approximation of $y(\mathbf{x})$, the univariate ($S=1$), bivariate ($S=2$), and trivariate ($S=3$) approximations, $\tilde{y}_1(\mathbf{x})$, $\tilde{y}_2(\mathbf{x})$, and $\tilde{y}_3(\mathbf{x})$, respectively, provide two-, three-, and four-term approximants of the finite decomposition in Equation (1). Similarly, quadrivariate and other higher-variate approximations can be derived by appropriately selecting the value of S. The fundamental conjecture underlying this decomposition is that component functions arising in the function decomposition will exhibit insignificant S-variate effects cooperatively when $S \to N$, leading to useful lower-variate approximations of $y(\mathbf{x})$. When $S=N$, $\tilde{y}_1(\mathbf{x})$ converges to the exact function $y(\mathbf{x})$. In other words, Equation (2) generates a hierarchical and convergent sequence of approximations of $y(\mathbf{x})$.

The decomposition in Equation (1) can be traced to the work of Hoeffding [7] in the 1940s and is well known in the statistics literature as analysis of variance (ANOVA) [8]. This decomposition, later referred to as the high-dimensional model representation (HDMR), was subject to further refinements, leading to notable contributions in function approximations [9–11]. Recently, the author's group exploited this decomposition in calculating statistical moments of response [4] and reliability [5] of uncertain mechanical systems.

3. POLYNOMIAL DIMENSIONAL DECOMPOSITION METHOD

Let $(\Omega, \mathscr{F}, P)$ be a complete probability space, where Ω is a sample space, $\mathscr{F}$ is a σ-field on Ω, and $P: \mathscr{F} \to [0, 1]$ is a probability measure. With $\mathscr{B}^N$ representing the Borel σ-field on $\mathbb{R}^N$, consider an $\mathbb{R}^N$-valued independent random vector $\{\mathbf{X} = \{X_1, \ldots, X_N\}^{\mathrm{T}} : (\Omega, \mathscr{F}) \to (\mathbb{R}^N, \mathscr{B}^N)\}$ that describes

DOI: 10.1002/nme

statistical uncertainties in all coefficients of and input to the governing (algebraic, differential, and integral) equation of a given stochastic problem. The probability law of $\mathbf{X}$ is completely defined by the joint probability density function $f_{\mathbf{X}}(\mathbf{x}) = \prod_{i=1}^{i=N} f_i(x_i)$ that is associated with the probability measure P, where $f_i(x_i)$ is the probability density function of X_i with the probability measure P_i.

Let $y(\mathbf{X})$, a real-valued, measurable transformation on $(\Omega, \mathscr{F})$, define a relevant performance function of a stochastic system. In general, the multivariate function $y : \mathbb{R}^N \to \mathbb{R}$ is implicit, is not analytically available, and can be viewed only as a high-dimensional input–output mapping, where the evaluation of the output function y for a given input $\mathbf{x}$ requires expensive finite element, boundary element, or mesh-free analysis. Therefore, methods employed in stochastic analysis must be capable of generating accurate probabilistic characteristics of $y(\mathbf{X})$ with an acceptably small number of output function evaluations.

3.1. Orthonormal polynomial basis

Let X_i follow the probability density function $f_i(x_i)$ with support $[a_i, b_i] \subseteq \mathbb{R}$, where $-\infty \leqslant a_i < b_i \leqslant +\infty$. Consider a collection of univariate component functions on $[a_i, b_i]$ equipped with the measure $P_i(\mathrm{d}x_i) = f_i(x_i)\,\mathrm{d}x_i$, where $\mathrm{d}x_i$ is the Lebesgue measure. Denote the space of square-integrable functions with the measure P_i as

$$\mathscr{L}_2(\Omega_i, \mathscr{F}_i, P_i) := \left\{ y_i(x_i) : \int_{a_i}^{b_i} y_i^2(x_i) f_i(x_i)\,\mathrm{d}x_i < \infty \right\} \tag{3}$$

where $(\Omega_i, \mathscr{F}_i, P_i)$ is the triple associated with the random variable X_i. The inner product of this space is defined as

$$(y_i, z_i)_{P_i} := \int_{a_i}^{b_i} y_i(x_i) z_i(x_i) f_i(x_i)\,\mathrm{d}x_i = \mathbb{E}_{P_i}[y_i(X_i) z_i(X_i)] \tag{4}$$

where $y_i(x_i)$ and $z_i(x_i)$ are any two univariate functions of x_i and $\mathbb{E}_{P_i}[y_i^2(X_i)] < \infty$ with $\mathbb{E}_{P_i}$ representing the expectation operator with respect to the probability measure P_i. Therefore, $\mathscr{L}_2(\Omega_i, \mathscr{F}_i, P_i)$ is a Hilbert space that can also be interpreted as the space of functions of random variables with finite second moments.

Consider a set of complete orthonormal bases in the Hilbert space $\mathscr{L}_2(\Omega_i, \mathscr{F}_i, P_i)$ and denote it by $\{\psi_j(x_i);\ j = 0, 1, \ldots\}$, which satisfies

$$\mathbb{E}_{P_i}[\psi_j(X_i)] = \int_{a_i}^{b_i} \psi_j(x_i) f_i(x_i)\,\mathrm{d}x_i = \begin{cases} 1 & \text{if } j = 0 \\ 0 & \text{if } j \neq 0 \end{cases} \tag{5}$$

and

$$\mathbb{E}_{P_i}[\psi_{j_1}(X_i)\psi_{j_2}(X_i)] = \int_{a_i}^{b_i} \psi_{j_1}(x_i)\psi_{j_2}(x_i) f_i(x_i)\,\mathrm{d}x_i = \begin{cases} 1 & \text{if } j_1 = j_2 \\ 0 & \text{if } j_1 \neq j_2 \end{cases} \tag{6}$$

i.e. the basis functions have a zero mean, unit variance (norm), and are mutually orthogonal for $j, j_1, j_2 \geqslant 1$. A broad range of polynomial basis functions satisfying Equations (5) and (6) can be constructed when the probability density of X_i is prescribed. Table I shows a few classical orthonormal polynomials, including Hermite, Legendre, and Jacobi polynomials, when X_i

DOI: 10.1002/nme

Table I. Classical Hermite, Legendre, and Jacobi orthogonal polynomials.

	Hermite	Legendre	Jacobi*
Symbol	$H_i(x),\ i=0,\ldots,\infty$	$L_i(x),\ i=0,\ldots,\infty$	$P_i(x;\alpha,\beta),\ i=0,\ldots,\infty, \alpha>-1, \beta>-1$
Support, $[a,b]$	$[-\infty,+\infty]$	$[-1,+1]$	$[-1,+1]$
Weight function, $w(x)$	$\exp(-x^2/2)$	1	$(1-x)^\alpha(1+x)^\beta$
Probability density function, $f(x)$	$\frac{\exp(-x^2/2)}{\sqrt{2\pi}}$ (Gaussian)	$\frac{1}{2}$ (Uniform)	$\frac{\Gamma(\alpha+\beta+2)(1-x)^\alpha(1+x)^\beta}{\Gamma(\alpha+1)\Gamma(\beta+1)2^{\alpha+\beta+1}}$ (Beta)
Differential equation	$H_i''-xH_i'+iH_i=0$	$(1-x^2)L_i''-2xL_i'+i(i+1)L_i=0$	$(1-x^2)P_i''-\beta-\alpha-(\alpha+\beta+2)xP_i'$ $+i(i+\alpha+\beta+1)P_i=0$
Rodrigues' formula	$H_i=\frac{(\mathrm{d}^i/\mathrm{d}x^i)[\exp(-ix^2/2)]}{(-1)^i\exp(-x^2/2)}$	$L_i=\frac{(\mathrm{d}^i/\mathrm{d}x^i)[(1-x^2)^i]}{(-1)^i2^i i!}$	$P_i=\frac{(\mathrm{d}^i/\mathrm{d}x^i)[(1-x)^{i+\alpha}(1+x)^{i+\beta}]}{(-1)^i2^i i!(1-x)^\alpha(1+x)^\beta}$
Recurrence relation	$H_{i+1}=xH_i-iH_{i-1}$	$(i+1)L_{i+1}=(2i+1)xL_i-iL_{i-1}$	$2(i+1)(i+\alpha+\beta+1)(2i+\alpha+\beta)P_{i+1}$ $=[(2i+\alpha+\beta+1)(\alpha^2-\beta^2)$ $+(2i+\alpha+\beta)_3x]P_i-2(i+\alpha)$ $\times(i+\beta)(2i+\alpha+\beta+2)P_{i-1}$
Orthogonality w.r.t.: density	$\int_{-\infty}^{+\infty}H_i(x)H_j(x)f(x)\,\mathrm{d}x=i!\delta_{ij}$	$\int_{-\infty}^{+\infty}L_i(x)L_j(x)f(x)\,\mathrm{d}x=\frac{1}{2i+1}\delta_{ij}$	$\int_{-\infty}^{+\infty}P_i(x;\alpha,\beta)P_j(x;\alpha,\beta)f(x)\,\mathrm{d}x$ $=\frac{2^{\alpha+\beta+1}}{2i+\alpha+\beta+1}\frac{\Gamma(i+\alpha+1)\Gamma(i+\beta+1)}{i!\Gamma(i+\alpha+\beta+1)}$ $\times\frac{\Gamma(\alpha+\beta+2)}{\Gamma(\alpha+1)\Gamma(\beta+1)2^{\alpha+\beta+1}}\delta_{ij}$

Int. J. Numer. Meth. Engng 2008; **76**:2091–2116
DOI: 10.1002/nme

Table I. *Continued.*

	Hermite	Legendre	Jacobi*
First four polynomials	$H_0 = 1$	$L_0 = 1$	$P_0 = 1$
	$H_1(x) = x$	$L_1(x) = x$	$P_1(x; 3, 3) = 4x$
	$H_2(x) = x^2 - 1$	$L_2(x) = (3x^2 - 1)/2$	$P_2(x; 3, 3) = (45x^2 - 5)/5$
	$H_3(x) = x^3 - 3x$	$L_3(x) = (5x^3 - 3x)/2$	$P_3(x; 3, 3) = (220x^3 - 60x)/8$
			$P_0 = 1$
			$P_1(x; 1, 1) = 2x$
			$P_2(x; 1, 1) = (15x^2 - 3)/4$
			$P_3(x; 1, 1) = (56x^3 - 24x)/8$

*The Pochhammer symbol $(x)_n := x(x+1)(x+2)\cdots(x+n-1) = (\Gamma(x+n))/\Gamma(x)$.

DOI: 10.1002/nme

follows Gaussian, Uniform, and Beta probability distributions, respectively. A more extensive list of orthogonal polynomials is available elsewhere [12].

3.2. Fourier-polynomial expansions

The polynomials $\{\psi_j(x_i);\ j=0,1,\ldots\}$ form an orthonormal basis in $\mathscr{L}_2(\Omega_i, \mathscr{F}_i, P_i)$. Therefore, for any zero-mean univariate random function $y_i(X_i) \in \mathscr{L}_2(\Omega_i, \mathscr{F}_i, P_i)$ with $\mathbb{E}_{P_i}[y_i^2(X_i)] < \infty$, there exists a Fourier-polynomial expansion

$$y_i(x_i) = \sum_{j=1}^{\infty} \alpha_{ij} \psi_j(x_i) \tag{7}$$

where $\alpha_{ij} := \int_{a_i}^{b_i} y_i(x_i)\psi_j(x_i) f_i(x_i)\,\mathrm{d}x_i$ for $i=1,\ldots,N$ and $j=1,\ldots,\infty$ is a coefficient associated with the jth basis function expressed in terms of the ith variable.

The Fourier-polynomial expansion can be easily extended to multiple dimensions. For a finite index $\mathbf{J}_S = \{j_1,\ldots,j_S\}$ with non-negative integers and $S=1,\ldots,N$, define a multivariate polynomial by the tensor product

$$\psi_{\mathbf{J}_S}(x_{i_1},\ldots,x_{i_S}) = \prod_{k=1}^{S} \psi_{j_k}(x_{i_k}) \tag{8}$$

and a product probability space $(\overline{\Omega}_S, \overline{\mathscr{F}}_S, \overline{P}_S)$, where $\overline{\Omega}_S = \times_{k=1}^{k=S} \Omega_k$ is the product sample space, $\overline{\mathscr{F}}_S = \bigotimes_{k=1}^{k=S} \mathscr{F}_k$ is the associated product σ-field, and $\overline{P}_S = \bigotimes_{k=1}^{k=S} P_k$ is the associated product probability measure. Then, $\{\psi_{\mathbf{J}_S}(x_{i_1},\ldots,x_{i_S})\}$ constitutes an orthonormal polynomial basis in the Hilbert space $\mathscr{L}_2(\overline{\Omega}_S, \overline{\mathscr{F}}_S, \overline{P}_S)$. Suppose $y_{i_1\cdots i_S}(x_{i_1},\ldots,x_{i_S})$ is an S-variate component function such that $\mathbb{E}_{\overline{P}_S}[y^2_{i_1\cdots i_S}(X_{i_1},\ldots,X_{i_S})] < \infty$, where the expectation operator $\mathbb{E}_{\overline{P}_S}$ is associated with $\overline{P}_S$; then $y_{i_1\cdots i_S}(X_{i_1},\ldots,X_{i_S}) \in \mathscr{L}_2(\overline{\Omega}_S, \overline{\mathscr{F}}_S, \overline{P}_S)$. Therefore, there exists a Fourier-polynomial expansion

$$y_{i_1\cdots i_S}(x_{i_1},\ldots,x_{i_S}) = \sum_{j_S=1}^{\infty} \cdots \sum_{j_1=1}^{\infty} C_{i_1\cdots i_S j_1\cdots j_S} \prod_{k=1}^{S} \psi_{j_k}(x_{i_k}) \tag{9}$$

where

$$C_{i_1\cdots i_S j_1\cdots j_S} = \int_{\mathbb{A}^S} y_{i_1\cdots i_S}(x_{i_1},\ldots,x_{i_S}) \prod_{k=1}^{S} \psi_{j_k}(x_{i_k}) f_k(x_k)\,\mathrm{d}x_k \tag{10}$$

is a coefficient associated with the product of j_1 through j_S basis functions expressed in terms of $x_{i_1},\ldots,x_{i_S}$ and $\mathbb{A}^S = \times_{i=1}^{i=S}[a_i, b_i]$ is a rectangle in $\mathbb{R}^S$. The expansion is valid for any finite-dimensional space $\mathscr{L}_2(\overline{\Omega}_S, \overline{\mathscr{F}}_S, \overline{P}_S)$ with $1 \leqslant S \leqslant N$. In other words, Equations (9) and (10) can represent all component functions of the multivariate function decomposition in Equation (1). Furthermore, for any two integers $S \neq T$, if the chosen basis functions satisfy

$$\int_{\mathbb{A}^N} \psi_{\mathbf{J}_S}(x_{i_1},\ldots,x_{i_S}) \psi_{\mathbf{J}_T}(x_{i_1},\ldots,x_{i_T}) f_{\mathbf{X}}(\mathbf{x})\,\mathrm{d}\mathbf{x} = 0 \tag{11}$$

the component functions $y_{i_1\cdots i_S}(x_{i_1},\ldots,x_{i_S})$ and $y_{i_1\cdots i_T}(x_{i_1},\ldots,x_{i_T})$ will preserve their orthogonality in the decomposition presented in Equation (1).

DOI: 10.1002/nme

The Fourier-polynomial expansion in Equation (9) is an infinite series. In practice, it must be truncated, say, by m terms in each variable, yielding the Fourier-polynomial approximation

$$y_{i_1\cdots i_S}(x_{i_1},\ldots,x_{i_S}) \cong \sum_{j_S=1}^{m}\cdots\sum_{j_1=1}^{m} C_{i_1\cdots i_S j_1\cdots j_S}\prod_{k=1}^{S}\psi_{j_k}(x_{i_k}) \tag{12}$$

which approaches $y_{i_1\cdots i_S}(x_{i_1},\ldots,x_{i_S})$ in the mean square sense as $m\to\infty$. The approximation converges very fast if the component function $y_{i_1\cdots i_S}(x_{i_1},\ldots,x_{i_S})$ is very smooth. However, the convergence rate can be quite complicated in general. For a specific polynomial approximation, such as the Fourier–Hermite approximation, a nice overview of convergence properties is available in Boyd's textbook [13].

3.3. Formulation of coefficients

An important feature of the decomposition in Equation (1) is the selection of the constant y_0 and component functions $y_{i_1\cdots i_S}(x_{i_1},\ldots,x_{i_S})$, $S=1,\ldots,N$. By defining an error functional associated with a given $y(\mathbf{x})$, an appropriate kernel function, and the domain of $\mathbf{x}$, an optimization problem can be formulated and solved to obtain the desired component functions. However, different kernel functions will create distinct, yet formally equivalent, decompositions, all exhibiting the same structure as Equation (1). In particular, the ANOVA decomposition containing densities of $\{X_{i_1},\ldots,X_{i_S}\}^{\mathrm{T}}$ as the kernel function leads to [9]

$$\begin{aligned}
y_0 &:= \int_{\mathbb{A}^N} y(\mathbf{x}) f_{\mathbf{X}}(\mathbf{x})\,\mathrm{d}\mathbf{x} = \mathbb{E}_P[y(\mathbf{X})]\\
y_i(x_i) &:= \int_{\mathbb{A}^{N-1}} y(\mathbf{x})\prod_{k\neq i} f_k(x_k)\,\mathrm{d}x_k - y_0\\
y_{i_1 i_2}(x_{i_1},x_{i_2}) &:= \int_{\mathbb{A}^{N-2}} y(\mathbf{x})\prod_{k\notin\{i_1,i_2\}} f_k(x_k)\,\mathrm{d}x_k - y_{i_1}(x_{i_1}) - y_{i_2}(x_{i_2}) - y_0\\
&\vdots\ \vdots\ \vdots\\
y_{i_1\cdots i_S}(x_{i_1},\ldots,x_{i_S}) &:= \int_{\mathbb{A}^{N-S}} y(\mathbf{x})\prod_{k\notin\{i_1,\ldots,i_S\}} f_k(x_k)\,\mathrm{d}x_k\\
&\quad - \sum_{k_1<\cdots<k_{S-1}\subset\{i_1,\ldots,i_S\}} y_{k_1\cdots k_{S-1}}(x_{k_1},\ldots,x_{k_{S-1}})\\
&\quad - \sum_{k_1<\cdots<k_{S-2}\subset\{i_1,\ldots,i_S\}} y_{k_1\cdots k_{S-2}}(x_{k_1},\ldots,x_{k_{S-2}})\\
&\quad - \cdots - \sum_{k} y_{i_k}(x_{i_k}) - y_0
\end{aligned} \tag{13}$$

where $\mathbb{E}_P$ is the expectation operator with respect to P. Substituting the last expression of Equation (13) into Equation (10) and then employing the orthogonality condition for basis functions yields

$$C_{i_1\cdots i_S j_1\cdots j_S} := \int_{\mathbb{A}^N} y(\mathbf{x})\prod_{k=1}^{S}\psi_{j_k}(x_{i_k}) f_{\mathbf{X}}(\mathbf{x})\,\mathrm{d}\mathbf{x} = \mathbb{E}_P\left[y(\mathbf{X})\prod_{k=1}^{S}\psi_{j_k}(X_{i_k})\right] \tag{14}$$

DOI: 10.1002/nme

from which all coefficients of the Fourier-polynomial approximations of component functions can be derived. For example, setting $S=1$, 2, and 3, the univariate, bivariate, and trivariate component functions, respectively, are

$$y_i(x_i) \cong \sum_{j=1}^{m} \alpha_{ij}\psi_j(x_i) \tag{15}$$

$$y_{i_1 i_2}(x_{i_1}, x_{i_2}) \cong \sum_{j_2=1}^{m}\sum_{j_1=1}^{m} \beta_{i_1 i_2 j_1 j_2}\psi_{j_1}(x_{i_1})\psi_{j_2}(x_{i_2}) \tag{16}$$

and

$$y_{i_1 i_2 i_3}(x_{i_1}, x_{i_2}, x_{i_3}) \cong \sum_{j_3=1}^{m}\sum_{j_2=1}^{m}\sum_{j_1=1}^{m} \gamma_{i_1 i_2 i_3 j_1 j_2 j_3}\psi_{j_1}(x_{i_1})\psi_{j_2}(x_{i_2})\psi_{j_3}(x_{i_3}) \tag{17}$$

where

$$\alpha_{ij} := \int_{\mathbb{A}^N} y(\mathbf{x})\psi_j(x_i) f_{\mathbf{X}}(\mathbf{x})\,\mathrm{d}\mathbf{x} = \mathbb{E}_P[y(\mathbf{X})\psi_j(X_i)] \tag{18}$$

$$\beta_{i_1 i_2 j_1 j_2} := \int_{\mathbb{A}^N} y(\mathbf{x})\psi_{j_1}(x_{i_1})\psi_{j_2}(x_{i_2}) f_{\mathbf{X}}(\mathbf{x})\,\mathrm{d}\mathbf{x} = \mathbb{E}_P[y(\mathbf{X})\psi_{j_1}(X_{i_1})\psi_{j_2}(X_{i_2})] \tag{19}$$

and

$$\begin{aligned}\gamma_{i_1 i_2 i_3 j_1 j_2 j_3} &:= \int_{\mathbb{A}^N} y(\mathbf{x})\psi_{j_1}(x_{i_1})\psi_{j_2}(x_{i_2})\psi_{j_3}(x_{i_3}) f_{\mathbf{X}}(\mathbf{x})\,\mathrm{d}\mathbf{x} \\ &= \mathbb{E}_P[y(\mathbf{X})\psi_{j_1}(X_{i_1})\psi_{j_2}(X_{i_2})\psi_{j_3}(X_{i_3})]\end{aligned} \tag{20}$$

are the corresponding coefficients. The calculation of these coefficients requires evaluating N-dimensional integrals over the entire domain of $\mathbf{X}$. For large N, direct numerical integration to calculate these coefficients is prohibitive and is, therefore, ruled out. It is worth noting that similar integrals appear in the polynomial chaos expansion method [14, 15], where the coefficients are commonly estimated by Galerkin-based methods [15], sampling methods [16], and others [17]. In this study, an alternative method entailing dimension-reduction integration of a multivariate function was employed to determine the coefficients.

A similar expansion adopting the shifted Legendre polynomials of scaled variables as the orthonormal basis has been reported in conjunction with the random sampling HDMR [11]. In contrast, the Fourier-polynomial expansion presented in this study does not require any scaling of variables and can accommodate a host of orthonormal polynomials that are consistent with the probability measure of a random variable.

3.4. Dimension-reduction integration for calculating coefficients

Following an early idea by Xu and Rahman [4], consider a lower-variate approximation of the N-variate function $y(\mathbf{x})$, which results in lower-dimensional integrations for evaluating an N-dimensional integral, leading to the coefficients. Let $\mathbf{c}=\{c_1,\ldots,c_N\}^{\mathrm{T}}$ be the mean value of $\mathbf{X}$ and $y(c_1,\ldots,c_{k_1-1},x_{k_1},c_{k_1+1},\ldots,c_{k_{R-k}-1},x_{k_{R-k}},c_{k_{R-k}+1},\ldots,c_N)$ represent an $(R-k)$th dimensional

DOI: 10.1002/nme

component function of $y(\mathbf{x})$, where $S \leqslant R \leqslant N$ and $k = 0, \ldots, R$. For example, when $R = 1$, the zero-dimensional component function, which is a constant, is $y(\mathbf{c})$ and the one-dimensional component functions are $y(x_1, c_2, \ldots, c_N)$, $y(c_1, x_2, \ldots, c_N), \ldots, y(c_1, c_2, \ldots, x_N)$. Using Xu and Rahman's multivariate function theorem [4], it can be shown that a special R-variate approximation of $y(\mathbf{x})$, defined by

$$\hat{y}_R(\mathbf{x}) := \sum_{k=0}^{R} (-1)^k \binom{N-R+k-1}{k} \times \sum_{k_1,\ldots,k_{R-k}=1; k_1<\cdots<k_{R-k}}^{N} \times y(c_1, \ldots, c_{k_1-1}, x_{k_1}, c_{k_1+1}, \ldots, c_{k_{R-k}-1}, x_{k_{R-k}}, c_{k_{R-k}+1}, \ldots, c_N) \tag{21}$$

consists of all terms of the Taylor series of $y(\mathbf{x})$ that have less than or equal to R variables. The expanded form of Equation (21), when compared with the Taylor expansion of $y(\mathbf{x})$, indicates that the residual error in $\hat{y}_R(\mathbf{x})$ includes terms of dimensions $R+1$ and higher. All higher-order R- and lower-variate terms of $y(\mathbf{x})$ are included in Equation (21), which should therefore generally provide a higher-order approximation of a multivariate function than equations derived from first- or second-order Taylor expansions. Therefore, for $R < N$, an N-dimensional integral can be efficiently estimated by at most R-dimensional integrations, if the contributions from terms of dimensions $R+1$ and higher are negligible.

Substituting $y(\mathbf{x})$ in Equations (13) (first line) and (14) by $\hat{y}_R(\mathbf{x})$, the coefficients can be estimated from

$$y_0 \cong \sum_{k=0}^{R} (-1)^k \binom{N-R+k-1}{k} \sum_{k_1,\ldots,k_{R-k}=1; k_1<\cdots<k_{R-k}}^{N} \times \int_{\mathbb{A}^{R-k}} y(c_1, \ldots, c_{k_1-1}, x_{k_1}, c_{k_1+1}, \ldots, c_{k_{R-k}-1}, x_{k_{R-k}}, c_{k_{R-k}+1}, \ldots, c_N) \times \prod_{m=1}^{R-k} f_{k_m}(x_{k_m})\, \mathrm{d}x_{k_m} \tag{22}$$

and

$$C_{i_1\cdots i_S j_1 \cdots j_S} \cong \sum_{k=0}^{R} (-1)^k \binom{N-R+k-1}{k} \sum_{k_1,\ldots,k_{R-k}=1; k_1<\cdots<k_{R-k}}^{N} \times \int_{\mathbb{A}^{R-k}} y(c_1, \ldots, c_{k_1-1}, x_{k_1}, c_{k_1+1}, \ldots, c_{k_{R-k}-1}, x_{k_{R-k}}, c_{k_{R-k}+1}, \ldots, c_N) \times \prod_{m=1}^{S} \psi_{j_m}(x_{i_m}) \prod_{m=1}^{R-k} f_{k_m}(x_{k_m})\, \mathrm{d}x_{k_m} \tag{23}$$

which require evaluating at most R-dimensional integrals. The proposed equations, Equations (22) and (23), are substantially simpler and more efficient than performing one N-dimensional integration, as in Equations (13) and (14), particularly when $R \ll N$. Hence, the computational effort in calculating the coefficients is significantly lowered using the dimension-reduction integration. When $R = 1$, 2, or 3, Equations (22) and (23) involve one-, at most two-, and at most three-dimensional

DOI: 10.1002/nme

integrations, respectively. Nonetheless, numerical integration is still required for a general function y. The integration points and associated weights depend on the probability distribution of X_i. They are readily available as Gauss–Hermite, Gauss–Legendre, and Gauss–Jacobi quadrature rules when a random variable follows Gaussian, Uniform, and Beta distributions, respectively [12]. For an arbitrary probability distribution of X_i, see the author's past work [18].

In performing the dimension-reduction integration, the value of R should be selected in such a manner that it is either equal to or greater than the value of S, which defines the truncation of Equation (1). Then all coefficients of S- or lower-variate approximations of $y(\mathbf{x})$ will have non-trivial solutions. For example, when $R=3$ and $N\geqslant 3$, Equation (21) yields

$$\begin{aligned}\hat{y}_3(\mathbf{x}) \cong & \sum_{k_1=1}^{N-2}\sum_{k_2=k_1+1}^{N-1}\sum_{k_3=k_2+1}^{N} \\ & \times y(c_1,\ldots,c_{k_1-1},x_{k_1},c_{k_1+1},\ldots,c_{k_2-1},x_{k_2},c_{k_2+1},\ldots,c_{k_3-1},x_{k_3},c_{k_3+1},\ldots,c_N) \\ & -(N-3)\sum_{k_1=1}^{N-1}\sum_{k_2=k_1+1}^{N} y(c_1,\ldots,c_{k_1-1},x_{k_1},c_{k_1+1},\ldots,c_{k_2-1},x_{k_2},c_{k_2+1},\ldots,c_N) \\ & +\frac{(N-2)(N-3)}{2}\sum_{k=1}^{N} y(c_1,\ldots,c_{k-1},x_k,c_{k+1},\ldots,c_N) \\ & -\frac{(N-1)(N-2)(N-3)}{6}y(\mathbf{c}) \end{aligned} \tag{24}$$

Correspondingly, Equations (22) and (23) lead to non-trivial expressions of the coefficients

$$\begin{aligned} y_0 \cong & \sum_{k_1=1}^{N-2}\sum_{k_2=k_1+1}^{N-1}\sum_{k_3=k_2+1}^{N} \\ & \times \int_{\mathbb{A}^3} y(c_1,\ldots,c_{k_1-1},x_{k_1},c_{k_1+1},\ldots,c_{k_2-1},x_{k_2},c_{k_2+1},\ldots,c_{k_3-1},x_{k_3},c_{k_3+1},\ldots,c_N) \\ & \times \prod_{m=1}^{3} f_{k_m}(x_{k_m})\,\mathrm{d}x_{k_m} - (N-3)\sum_{k_1=1}^{N-1}\sum_{k_2=k_1+1}^{N} \\ & \times \int_{\mathbb{A}^2} y(c_1,\ldots,c_{k_1-1},x_{k_1},c_{k_1+1},\ldots,c_{k_2-1},x_{k_2},c_{k_2+1},\ldots,c_N)\prod_{m=1}^{2} f_{k_m}(x_{k_m})\,\mathrm{d}x_{k_m} \\ & +\frac{(N-2)(N-3)}{2}\sum_{k=1}^{N}\int_{\mathbb{A}^1} y(c_1,\ldots,c_{k-1},x_k,c_{k+1},\ldots,c_N)\,f_k(x_k)\,\mathrm{d}x_k \\ & -\frac{(N-1)(N-2)(N-3)}{6}y(\mathbf{c}) \end{aligned} \tag{25}$$

DOI: 10.1002/nme

$$\alpha_{ij} \cong \sum_{k_1=1}^{N-2} \sum_{k_2=k_1+1}^{N-1} \sum_{k_3=k_2+1}^{N} \times \int_{\mathbb{A}^3} y(c_1, \ldots, c_{k_1-1}, x_{k_1}, c_{k_1+1}, \ldots, c_{k_2-1}, x_{k_2}, c_{k_2+1}, \ldots, c_{k_3-1}, x_{k_3}, c_{k_3+1}, \ldots, c_N) \times \psi_j(x_i) \prod_{m=1}^{3} f_{k_m}(x_{k_m})\, \mathrm{d}x_{k_m} - (N-3) \sum_{k_1=1}^{N-1} \sum_{k_2=k_1+1}^{N} \times \int_{\mathbb{A}^2} y(c_1, \ldots, c_{k_1-1}, x_{k_1}, c_{k_1+1}, \ldots, c_{k_2-1}, x_{k_2}, c_{k_2+1}, \ldots, c_N) \psi_j(x_i) \times \prod_{m=1}^{2} f_{k_m}(x_{k_m})\, \mathrm{d}x_{k_m} + \frac{(N-2)(N-3)}{2} \times \int_{\mathbb{A}^1} y(c_1, \ldots, c_{i-1}, x_i, c_{i+1}, \ldots, c_N) \psi_j(x_i) f_i(x_i)\, \mathrm{d}x_i \tag{26}$$

$$\beta_{i_1 i_2 j_1 j_2} \cong \sum_{k_1=1}^{N-2} \sum_{k_2=k_1+1}^{N-1} \sum_{k_3=k_2+1}^{N} \times \int_{\mathbb{A}^3} y(c_1, \ldots, c_{k_1-1}, x_{k_1}, c_{k_1+1}, \ldots, c_{k_2-1}, x_{k_2}, c_{k_2+1}, \ldots, c_{k_3-1}, x_{k_3}, c_{k_3+1}, \ldots, c_N) \times \prod_{m=1}^{2} \psi_{j_m}(x_{i_m}) \prod_{m=1}^{3} f_{k_m}(x_{k_m})\, \mathrm{d}x_{k_m} - (N-3) \times \int_{\mathbb{A}^2} y(c_1, \ldots, c_{i_1-1}, x_{i_1}, c_{i_1+1}, \ldots, c_{i_2-1}, x_{i_2}, c_{i_2+1}, \ldots, c_N) \times \prod_{m=1}^{2} \psi_{j_m}(x_{i_m}) f_{i_m}(x_{i_m})\, \mathrm{d}x_{i_m} \tag{27}$$

$$\gamma_{i_1 i_2 i_3 j_1 j_2 j_3} \cong \int_{\mathbb{A}^3} y(c_1, \ldots, c_{i_1-1}, x_{i_1}, c_{i_1+1}, \ldots, c_{i_2-1}, x_{i_2}, c_{i_2+1}, \ldots, c_{i_3-1}, x_{i_3}, c_{i_3+1}, \ldots, c_N) \times \prod_{m=1}^{3} \psi_{j_m}(x_{i_m}) f_{i_m}(x_{i_m})\, \mathrm{d}x_{i_m} \tag{28}$$

whereas the remaining coefficients associated with higher than trivariate component functions are *zero*. Therefore, the coefficients in Equations (25)–(28), which require at most three-dimensional integrations, can be used only for the univariate $[\tilde{y}_1(\mathbf{x})]$, bivariate $[\tilde{y}_2(\mathbf{x})]$, and trivariate $[\tilde{y}_3(\mathbf{x})]$ approximations of $y(\mathbf{x})$. If only the univariate or bivariate approximations of $y(\mathbf{x})$ are desired, it is possible to select $R=1$ or 2, thereby requiring only one-dimensional and at most two-dimensional integrations. The latter choice of R significantly reduces the computational effort, because

DOI: 10.1002/nme

of a lower-dimensional integration in estimating the corresponding coefficients. The impact of R will be numerically evaluated in the example section.

3.5. Computational flow and effort

From Equations (2) and (13)–(20), an S-variate approximation of the polynomial dimensional decomposition of $y(\mathbf{X})$ is

$$\tilde{y}_S(\mathbf{X}) \cong y_0 + \sum_{i=1}^{N}\sum_{j=1}^{m}\alpha_{ij}\psi_j(X_i) + \sum_{i_1,i_2=1;i_1<i_2}^{N}\sum_{j_2=1}^{m}\sum_{j_1=1}^{m}\beta_{i_1i_2j_1j_2}\psi_{j_1}(X_{i_1})\psi_{j_2}(X_{i_2}) + \sum_{i_1,i_2,i_3=1;i_1<i_2<i_3}^{N}\sum_{j_3=1}^{m}\sum_{j_2=1}^{m}\sum_{j_1=1}^{m}\gamma_{i_1i_2i_3j_1j_2j_3}\psi_{j_1}(X_{i_1})\psi_{j_2}(X_{i_2})\psi_{j_3}(X_{i_3}) + \cdots + \sum_{i_1,\ldots,i_S=1;i_1<\cdots<i_S}^{N}\sum_{j_S=1}^{m}\cdots\sum_{j_1=1}^{m}C_{i_1\cdots i_Sj_1\cdots j_S}\prod_{k=1}^{S}\psi_{j_k}(X_{i_k}) \tag{29}$$

which, for $S=N$, converges to $y(\mathbf{X})$ in the mean square sense as $m\to\infty$. The embedded coefficients, defined by Equations (13), (14), and (18)–(20), can be estimated by lower-dimensional numerical integrations, described by Equations (22) and (23). Once these coefficients are calculated, Equation (29) furnishes an approximate but explicit map $\tilde{y}_S:\mathbb{R}^N\to\mathbb{R}$ that can be viewed as a surrogate of the exact map $y:\mathbb{R}^N\to\mathbb{R}$ on $(\Omega,\mathscr{F})$. Therefore, any probabilistic characteristic of $y(\mathbf{X})$, including its statistical moments and probability density function, can be easily estimated by performing Monte Carlo simulation of $\tilde{y}_S(\mathbf{X})$. Figure 1 shows the computational flow for constructing $\tilde{y}_S(\mathbf{X})$.

The S-variate approximation of the decomposition method requires evaluation of the deterministic coefficients y_0 and $C_{i_1\cdots i_Sj_1\cdots j_S}$. If these coefficients are estimated by at most the R-dimensional ($R\geqslant S\geqslant 1$) numerical integration with an n-point quadrature rule in Equations (22) and (23), the following deterministic responses (function evaluations) are required: $y(\mathbf{c})$, $y(c_1,\ldots,c_{k_1-1},x_{k_1}^{(j_1)},c_{k_1+1},\ldots,c_{k_R-1},x_{k_R}^{(j_R)},c_{k_R+1},\ldots,c_N)$ for $k_1,\ldots,k_R=1,\ldots,N$ and $j_1,\ldots,j_R=1,\ldots,n$, where the superscripts on variables indicate the corresponding integration points. Therefore, the total cost for an S-variate polynomial dimensional decomposition entails a maximum of $\sum_{k=0}^{k=R}\binom{N}{R-k}n^{R-k}$ function evaluations. If the integration points include a common point in each coordinate x_i (see the forthcoming example section), the numbers of function evaluations reduce to $\sum_{k=0}^{k=R}\binom{N}{R-k}(n-1)^{R-k}$. In the latter case, for example, the univariate ($S=R=1$), bivariate ($S=R=2$), and trivariate ($S=R=3$) approximations require $(n-1)N+1$, $N(N-1)(n-1)^2/2+(n-1)N+1$, and $N(N-1)(N-2)(n-1)^3/6+N(N-1)(n-1)^2/2+(n-1)N+1$ function evaluations, respectively.

Finally, the Monte Carlo simulation in the decomposition method should not be confused with the *direct* Monte Carlo simulation. The direct Monte Carlo simulation, which requires numerical calculations of $y(\mathbf{x}^{(l)})$ for a sample $\mathbf{x}^{(l)}$, can be expensive or even prohibitive, particularly when the sample size needs to be very large for estimating higher-order moments or small failure probabilities. In contrast, the Monte Carlo simulation embedded in the decomposition method requires evaluations of simple analytical functions that stem from an S-variate approximation $\tilde{y}_S(\mathbf{x}^{(l)}$ of $y(\mathbf{x}^{(l)})$. Therefore, an arbitrarily large sample size can be accommodated in the decomposition method.

DOI: 10.1002/nme

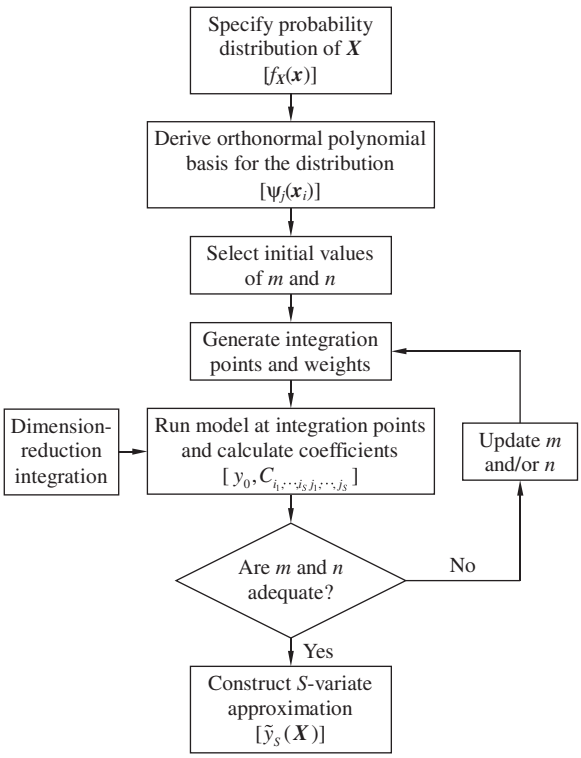

Figure 1. A flowchart for constructing an S-variate approximation of the polynomial dimensional decomposition method.

4. REMARKS

The Wiener polynomial chaos expansion of a stochastic response is [14, 15]

$$y = a_0 + \sum_{i_1=1}^{\infty} a_{i_1} H_1(U_{i_1}) + \sum_{i_1=1}^{\infty} \sum_{i_2=1}^{i_1} a_{i_1 i_2} H_2(U_{i_1}, U_{i_2}) + \sum_{i_1=1}^{\infty} \sum_{i_2=1}^{i_1} \sum_{i_3=1}^{i_2} a_{i_1 i_2 i_3} H_3(U_{i_1}, U_{i_2}, U_{i_3}) + \cdots \tag{30}$$

where $\{U_1, U_2, \ldots\}^{\mathrm{T}}$ is an infinite-dimensional standard Gaussian vector, $H_S(U_{i_1}, \ldots, U_{i_S})$ is an S-variate Hermite polynomial of order S, a_0 and $a_{i_1 \cdots i_S}$ are expansion coefficients, and $S = 1, \ldots, \infty$. Although a generalized version subsuming other types of random variables and orthogonal polynomials is available [19], several important observations can be made when comparing the dimensional decomposition and polynomial chaos expansion methods.

First, the dimensional decomposition is a finite sum that contains $2^N - 1$ number of summands and N random variables. In contrast, the polynomial chaos expansion is an infinite series and contains an infinite number of random variables. Therefore, if the component functions in

DOI: 10.1002/nme

Equation (1) are exact or the polynomial expansion of the component functions is convergent, the dimensional decomposition is exact or convergent.

Second, the terms in the polynomial chaos expansion are organized with respect to the order of polynomials. On the other hand, the dimensional decomposition is structured with respect to the degree of cooperativity between a finite number of random variables. If a response is highly non-linear but contains rapidly diminishing cooperative effects of multiple random variables, the dimensional decomposition is effective. This is because the lower-variate (univariate, bivariate, etc.) terms of the decomposition can be just as non-linear by selecting appropriate values of m in Equation (29). In contrast, many terms are required to be included in the polynomial chaos expansion to capture high non-linearity. However, if a response is lowly or mildly non-linear, is influenced by high-degree cooperativity of random variables, and the cooperative effects from a large number of variables are higher than those from a small number of variables, then nothing useful is gained from the dimensional decomposition. In the latter case, the polynomial chaos expansion is effective.

Third, the polynomial dimensional decomposition and polynomial chaos expansion methods are both convergent in the mean square sense. This is because of the inherent properties of orthogonal polynomials embedded in these methods. Further work is necessary to examine the convergence modes and properties of these methods when a stochastic response is discontinuous, non-smooth, or a function of mixed random variables with an arbitrary probability measure.

Finally, the polynomial dimensional decomposition can also be derived from the truncated polynomial chaos expansion. When the component functions in Equation (13), with $y(\mathbf{x})$ obtained from Equation (30), are substituted into Equation (2), the result is Equation (29). This relationship exists because of the common ingredient entailing Fourier-polynomial expansions in both methods. Nonetheless, the orderings of terms in these two methods are quite different. Therefore, significant differences exist regarding the accuracy, efficiency, and convergence properties of their truncated sum or series.

5. NUMERICAL EXAMPLES

Five numerical examples involving mathematical functions and solid mechanics problems are presented to illustrate the polynomial dimensional decomposition method for obtaining the probabilistic characteristics of response, including the tail distribution and reliability. The exact solution, when it exists, or direct Monte Carlo simulation, was employed to evaluate the accuracy, convergence, and computational efficiency of the decomposition method. The sample sizes for the direct Monte Carlo simulation and the embedded Monte Carlo simulation of the decomposition method varied from 10^6 in Examples 1–4 to 10^7 in Example 5, but they were identical for a specific problem. The expansion coefficients in Example 1 were calculated by exact numerical integration. For the remaining examples, the coefficients were estimated by the dimension-reduction integration. In Examples 2 and 3, a value of $R=3$ was selected, furnishing all required coefficients of the univariate to trivariate decomposition methods. Several values of $S \leqslant R \leqslant 3$ were selected in Example 4 to determine its impact, if any, on the result. In Example 5, R is identical to S, so that an S-variate decomposition method requires at most S-variate numerical integration. In Examples 3–5, all non-Gaussian random variables were transformed into Gaussian random variables. When comparing the computational efforts by various methods, the number of *original* performance function evaluations was chosen as the primary metric in this paper.

DOI: 10.1002/nme

5.1. Example 1: polynomial function

The first example involves a cubic polynomial

$$y(\mathbf{X}) = 50 - (X_1 + X_2)^3 + X_1 - X_2 - X_3 + X_1 X_2 X_3 - X_4 \tag{31}$$

where X_i, $i = 1-4$ are four independent and identically distributed random variables with mean $\mu_i = 0$ and standard deviation $\sigma_i = 1$. Four probability distributions of X_i were examined: (1) Gaussian or $N(0,1)$; (2) Uniform or $U(-\sqrt{3}, +\sqrt{3})$; (3) Beta or $B(-3, +3, 3, 3)$; and (4) Beta or $B(-\sqrt{5}, +\sqrt{5}, 1, 1)$. The respective probability densities, defined by

$$f_i(x_i) = \begin{cases} (1/\sqrt{2\pi})\exp(-x_i^2/2), \quad -\infty \leqslant x_i \leqslant +\infty & \text{Gaussian} \\ 1/(2\sqrt{3}), -\sqrt{3} \leqslant x_i \leqslant +\sqrt{3}; 0, \text{ o.w.} & \text{Uniform} \\ [\Gamma(8)/\{\Gamma^2(4)6^7\}](x_i+3)^3(3-x_i)^3, \\ \quad -3 \leqslant x_i \leqslant +3; 0, \text{ o.w.} & \text{Beta} \\ [\Gamma(4)/\{\Gamma^2(2)(2\sqrt{5})^3\}](x_i+\sqrt{5})(\sqrt{5}-x_i), \\ \quad -\sqrt{5} \leqslant x_i \leqslant +\sqrt{5}; 0, \text{ o.w.} & \text{Beta} \end{cases} \tag{32}$$

are plotted in Figure 2. The Hermite, Legendre, and Jacobi polynomials, listed in Table I, were normalized and then employed as complete orthonormal bases for probability measures associated with the Gaussian, Uniform, and Beta distributions, respectively. Since Equation (31) represents a third-order polynomial, a value of $m = 3$ should exactly reproduce y. In that case, the highest order of integrands for calculating the coefficients of the polynomial dimensional decomposition is 6. A four-point numerical integration—Gauss–Hermite, Gauss–Legendre, and Gauss–Jacobi quadratures for Gaussian, Uniform, and Beta distributions, respectively—should then provide exact values of the coefficients. In this example, the coefficients were calculated using $m = 3$ in Equation (12) and then numerically integrating Equations (13) x(first line) and 14 with $n = 4$. Therefore, the only source of error in a truncated polynomial dimensional decomposition is the selection of S.

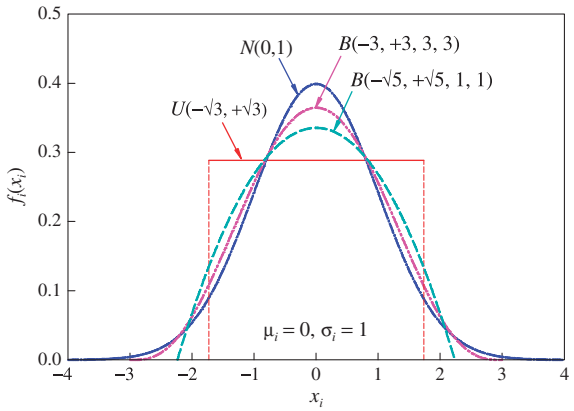

Figure 2. Gaussian, Uniform, and Beta probability densities of X_i.

DOI: 10.1002/nme

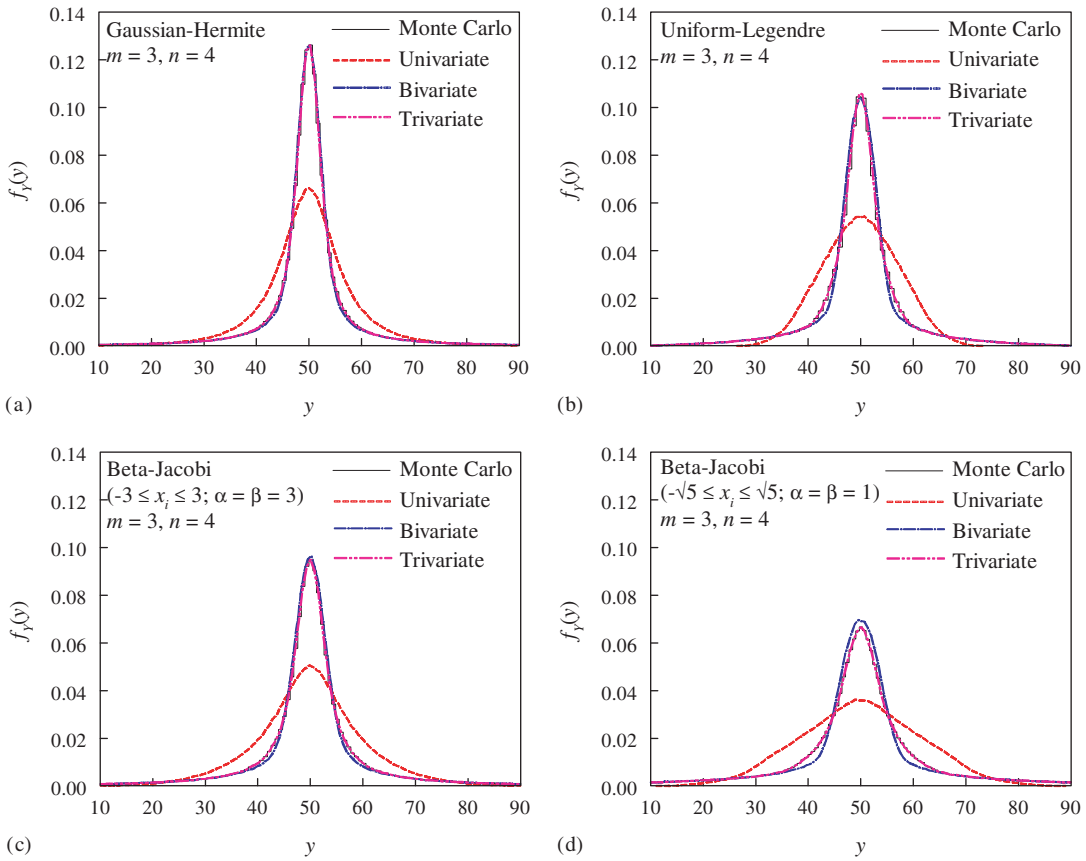

Figure 3. Probability densities of a polynomial function by various methods: (a) $X_i \sim N(0,1)$; (b) $X_i \sim U(-\sqrt{3},+\sqrt{3})$; (c) $X_i \sim B(-3,+3,3,3)$; and (d) $X_i \sim B(-\sqrt{5},+\sqrt{5},1,1)$.

Figures 3(a)–(d) and 4(a)–(d) show the probability densities and tail probability distributions, respectively, of $y(\mathbf{X})$ by several methods when the random variables follow Gaussian, Uniform, and two Beta distributions. Each of these figures contains four plots—one obtained from the direct Monte Carlo simulation and the remaining three generated from the univariate ($S=1$), bivariate ($S=2$), and trivariate ($S=3$) polynomial dimensional decomposition method. The probability densities and tail distributions converge rapidly with respect to S, regardless of the distribution of X_i. Compared with the direct Monte Carlo simulation, the univariate results are clearly inadequate. This is due to the absence of cooperative effects (mixed terms) of random variables in the univariate approximation. The bivariate solution, which captures cooperative effects of any two variables, is remarkably close to the Monte Carlo result. The probabilistic characteristics from the trivariate decomposition and Monte Carlo simulation are coincident, as $\tilde{y}_3(\mathbf{X})$ is identical to $y(\mathbf{X})$, which itself is a trivariate function. For the same reason, there is no need to pursue the quadrivariate approximation.

DOI: 10.1002/nme

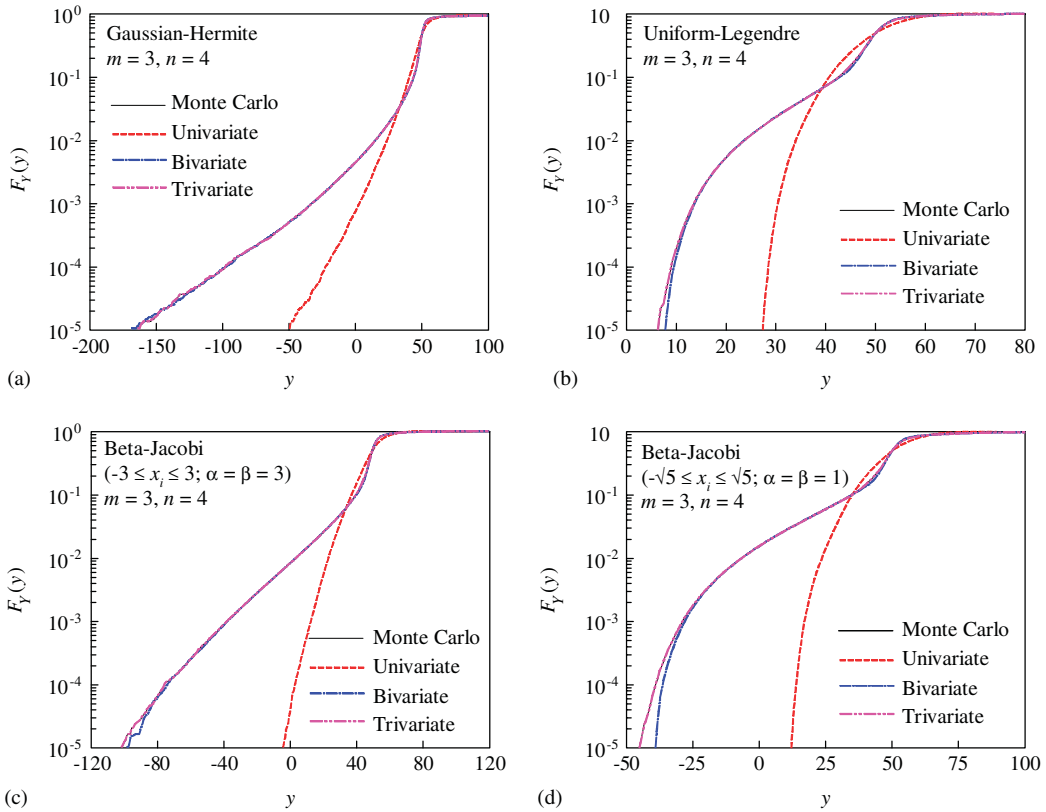

Figure 4. Tail probability distributions of a polynomial function by various methods: (a) $X_i \sim N(0,1)$; (b) $X_i \sim U(-\sqrt{3},+\sqrt{3})$; (c) $X_i \sim B(-3,+3,3,3)$; and (d) $X_i \sim B(-\sqrt{5},+\sqrt{5},1,1)$.

5.2. *Example 2: non-polynomial functions*

The objective of the second example is to illustrate the proposed decomposition method for non-polynomial performance functions, for instance, exponential and logarithmic functions. Two such functions are

$$y_1(\mathbf{X}) = 3 + \exp[-\tfrac{1}{4}(X_1 + 2X_2 + 3X_3)] - X_4 \tag{33}$$

and

$$y_2(\mathbf{X}) = \frac{1}{\sqrt{N}}\left[\sum_{i=1}^{N} -\ln\{\Phi(-X_i)\} - N\right] \tag{34}$$

where X_i, $i = 1, 2, \ldots$ are independent and identically distributed Gaussian random variables with mean $\mu_i = 0$ and standard deviation $\sigma_i = 1$, $\Phi(u) := (1/\sqrt{2\pi}) \int_{-\infty}^{u} \exp(-\xi^2/2)\,\mathrm{d}\xi$, and $N = 5$ or 15. Since these functions are non-polynomials, the orthonormal Hermite polynomials or any other polynomial basis for a finite value of m provides only an approximation. For the same reason, the coefficients, which involve Gauss–Hermite integrations of non-polynomials, can only be estimated for a finite value of n. Therefore, approximations in a truncated polynomial dimensional

DOI: 10.1002/nme

Table II. Results of $P[y_1(\mathbf{X})<0]$ in Example 2*.

m	n	Univariate	Bivariate	Trivariate
1	1	0	0	0
	2	2.34×10^{-3}	1×10^{-3}	9.88×10^{-4}
	3	4.62×10^{-3}	2.49×10^{-3}	2.5×10^{-3}
2	2	2.34×10^{-3}	1×10^{-3}	9.88×10^{-4}
	3	9.15×10^{-4}	1.89×10^{-4}	1.75×10^{-4}
	4	9.18×10^{-4}	1.96×10^{-4}	1.81×10^{-4}
3	3	9.15×10^{-4}	1.89×10^{-4}	1.75×10^{-4}
	4	7.81×10^{-4}	2.05×10^{-4}	1.91×10^{-4}
	5	8.02×10^{-4}	2.3×10^{-4}	2.15×10^{-4}
4	4	7.81×10^{-4}	2.05×10^{-4}	1.91×10^{-4}
	5	7.9×10^{-4}	1.77×10^{-4}	1.64×10^{-4}
	6	7.96×10^{-4}	1.76×10^{-4}	1.62×10^{-4}
5	5	7.9×10^{-4}	1.77×10^{-4}	1.64×10^{-4}
	6	7.83×10^{-4}	1.75×10^{-4}	1.64×10^{-4}
	7	7.83×10^{-4}	1.78×10^{-4}	1.63×10^{-4}

*$y_1(\mathbf{X})=3+\exp[-(X_1+2X_2+3X_3)/4]-X_4$.

decomposition of non-polynomials occur not only due to S but also due to m and n. In both performance functions, the coefficients were calculated using the dimension-reduction integration with $R=3$, i.e. by Equations (25)–(28).

Several combinations of $1\leqslant m\leqslant 5$ and $m\leqslant n\leqslant m+2$ and three values of $S=1$, 2, and 3 were employed to calculate the probability $P[y_1(\mathbf{X})<0]$ by the decomposition method. The calculated probabilities from the univariate, bivariate, and trivariate approximations are presented in Table II. The probabilities approach steady-state values when m and/or n increase, as expected. The bivariate and trivariate solutions are closer to the benchmark result of 1.61×10^{-4}, obtained from the direct Monte Carlo simulation.

The second performance function $y_2(\mathbf{X})$ is a non-linear but univariate function, regardless of N. Therefore, only the univariate decomposition method is needed. Using $m=1-3$ and $n=5$, Figures 5(a) and (b) display the tail probability distributions of $y_2(\mathbf{X})$ for $N=5$ and 15, respectively, by the univariate method. Since $y_2(\mathbf{X})$ follows a Gamma distribution, an exact solution exists and is also plotted in Figures 5(a) and (b). The univariate results derived from two or three Hermite polynomials are practically coincident with the exact distributions for both low-dimensional ($N=5$) and high-dimensional ($N=15$) problems.

5.3. Example 3: mixed random variables

Consider three stochastic problems with mixtures of Gaussian and non-Gaussian independent random variables, where the performance functions, described by

$$y_1(\mathbf{X}) = X_1X_2X_3X_4 - \tfrac{1}{8}X_5X_6^2 \tag{35}$$

$$y_2(\mathbf{X}) = 7.645\times10^{-4}X_1X_2\left(1-\frac{7.217\times10^{-3}X_2}{X_3}\right)-X_4-X_5 \tag{36}$$

DOI: 10.1002/nme

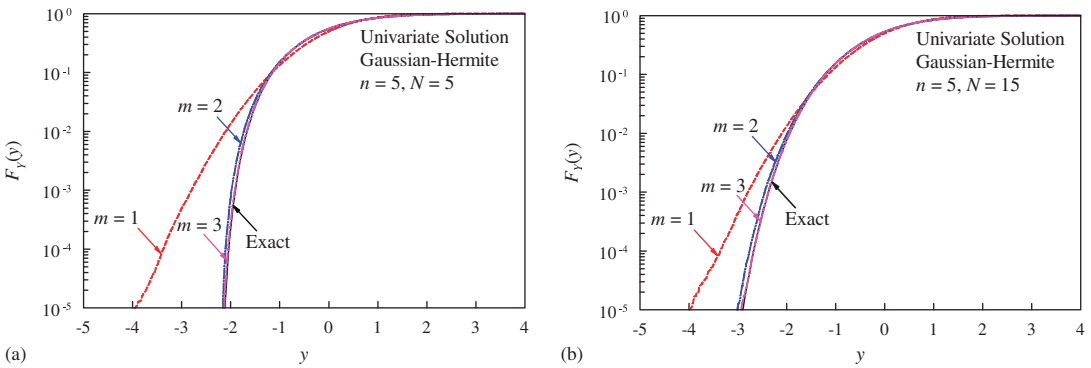

Figure 5. Tail probability distributions of two non-polynomial functions by various methods: (a) exponential function and (b) logarithmic function.

and

$$y_3(\mathbf{X}) = \sqrt{\frac{3X_1X_2(X_5 - X_6)}{X_4(2\pi X_3/60)^2(X_5^3 - X_6^3)}} - 0.37473 \tag{37}$$

were obtained from Melchers and Ahammed [20], Hong and Lind [21], and Penmetsa and Grandhi [22], respectively. The statistical properties and probability distributions of all random variables are described in Table III. The first problem contains a purely mathematical function, whereas the second and third problems are related to structural reliability analysis. The objective of each problem is to calculate the probability of failure, defined as $P[y_i(\mathbf{X}) < 0],\ i = 1, 2, 3$.

For random variables with arbitrary probability measures, several possibilities exist in defining a complete set of orthonormal polynomials. A direct approach is to construct one from scratch, which is consistent with the given probability distribution. However, an attractive alternative is to transform all original random variables into new random variables for which orthonormal polynomials are readily available. In this study, all non-Gaussian random variables were transformed into Gaussian random variables, so that Hermite polynomials can be used to approximate the mapped performance function in the Gaussian space.

The order of Hermite polynomials and the number of integration points were selected as follows: $m = 4$ and $n = 5$ for $y_1(\mathbf{X})$ and $y_2(\mathbf{X})$ and $m = 5$ and $n = 7$ for $y_3(\mathbf{X})$. Using these parameters, Table IV lists the estimated failure probabilities by the univariate, bivariate, and trivariate versions of the decomposition method and direct Monte Carlo simulation. The agreement between the predicted failure probabilities from all three versions, particularly the bivariate and trivariate versions, of the decomposition method and Monte Carlo simulation is excellent. It is worth noting that the univariate method, which underperformed in some of the previous examples, provided decent estimates of the failure probability in this example. This is because of the realistic performance functions and random variables chosen, where the individual effects of input variables are dominant over their cooperative effects.

The choice of transforming non-Gaussian variables to Gaussian variables, although a standard practice in the stochastic mechanics community, is somewhat arbitrary. Alternative transformations of original random variables into all-Uniform or all-Beta or other types of random variables are quite possible. The option remains whether the non-Gaussian variables are defined directly as an

DOI: 10.1002/nme

Table III. Statistical properties of mixed random variables in Example 3.

Performance function	Random variable	Mean	Standard deviation	Probability distribution
$y_1(\mathbf{X})$	X_1	4	0.1	Weibull
	X_2	25 000	2000	Lognormal
	X_3	0.875	0.1	Gumbel
	X_4	20	1	Uniform
	X_5	100	100	Exponential
	X_6	150	10	Gaussian
$y_2(\mathbf{X})$	X_1	1.01	0.0606	Gaussian
	X_2 (MPa)	400	40	Lognormal
	X_3 (MPa)	20	3.6	Gaussian
	X_4 (MN m)	95.87×10^{-3}	9.587×10^{-3}	Gaussian
	X_5 (MN m)	67.11×10^{-3}	16.78×10^{-3}	Gumbel
$y_3(\mathbf{X})$	X_1	0.9377	0.0459	Weibull
	X_2 (psi)	220 000	5000	Gaussian
	X_3 (rpm)	21 000	1000	Gaussian
	X_4 ($\mathrm{lb\,s^2/in^4}$)	$0.29/g^*$	$0.0058/g^*$	Uniform
	X_5 (in)	24	0.5	Gaussian
	X_6 (in)	8	0.3	Gaussian

*$g = 385.82\,\mathrm{in/s^2}$.

Table IV. Failure probabilities in Example 3.

Failure probability	Univariate	Bivariate	Trivariate	Monte Carlo
$P[y_1(\mathbf{X})<0]^*$	3.06×10^{-3}	3.42×10^{-3}	3.42×10^{-3}	3.42×10^{-3}
$P[y_2(\mathbf{X})<0]^\dagger$	3.52×10^{-3}	2.73×10^{-3}	2.73×10^{-3}	2.75×10^{-3}
$P[y_3(\mathbf{X})<0]^\ddagger$	1.58×10^{-3}	9.64×10^{-4}	9.66×10^{-4}	9.66×10^{-4}

*$y_1(\mathbf{X}) = X_1X_2X_3X_4 - \frac{1}{8}X_5X_6^2$.

†$y_2(\mathbf{X}) = 7.645\times10^{-4}X_1X_2\left(1 - \frac{7.217\times10^{-3}X_2}{X_3}\right) - X_4 - X_5$.

‡$y_3(\mathbf{X}) = \sqrt{\frac{3X_1X_2(X_5-X_6)}{X_4(2\pi X_3/60)^2(X_5^3-X_6^3)}} - 0.37473$.

input to a stochastic problem, as done here, or are derived from the discretization of a non-Gaussian random field, not considered in this study. Nonetheless, it would be interesting to study how a choice of transformation affects the smoothness of a performance function and to evaluate the accuracy and convergence properties of the resultant failure probability solution.

In all three examples presented so far, the performance functions are explicit and simple mathematical constructs. Two practical examples where a stochastic response is implicit and requires linear or non-linear finite element analysis via external commercial codes are demonstrated next.

5.4. Example 4: 10-bar truss

A linear-elastic, 10-bar truss, shown in Figure 6, is simply supported at nodes 1 and 4 and is subjected to two concentrated loads of 10^5 lb at nodes 2 and 3. The truss material is

DOI: 10.1002/nme

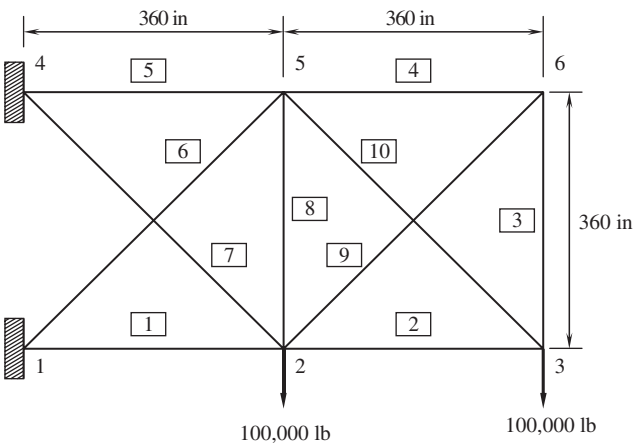

Figure 6. A 10-bar truss; a boxed or unboxed number indicates a member or node number.

made of an aluminum alloy with Young's modulus $E=10^7$ psi. The random input is $\mathbf{X}=\{X_1,\ldots,X_{10}\}^{\mathrm{T}}\in\mathbb{R}^{10}$, where X_i denotes the cross-sectional area of the ith bar. The random variables are independent and lognormally distributed with means $\mu_i=30\,\mathrm{in}^2$, $i=1,\ldots,10$, each of which has a 15% coefficient of variation. From a linear-elastic finite element analysis, the maximum vertical displacement $v_3(\mathbf{X})$ occurs at node 3, where the permissible displacement is limited to 1.7 in. The analysis also reveals that maximum axial stress $\sigma_1(\mathbf{X})$ occurs in member 1, where the allowable stress is 10 800 psi. The displacement- and stress-based performance functions,

$$y_1(\mathbf{X})=1.7-v_3(\mathbf{X}) \tag{38}$$

and

$$y_2(\mathbf{X})=10\,800-\sigma_1(\mathbf{X}) \tag{39}$$

were employed to define two component-level failure probabilities: $P_{F,1}:=P[y_1(\mathbf{X})<0]$ and $P_{F,2}:=P[y_2(\mathbf{X})<0]$ and a series system-level failure probability: $P_{F,3}:=P[\{y_1(\mathbf{X})<0\}\cup\{y_2(\mathbf{X})<0\}]$.

Table V presents two component failure probabilities and a system failure probability of the truss structure, calculated using the proposed univariate ($S=1$), bivariate ($S=2$), and trivariate ($S=3$) decomposition methods, and direct Monte Carlo simulation. For the decomposition method, $m=4$, $n=5$, and several values of $R=1$, 2, and 3 were selected. As can be seen from Table V, all three versions of the decomposition method, regardless of R, provide satisfactory to excellent predictions of these failure probabilities; yet, their required numbers of function evaluations are significantly less than that required by the Monte Carlo simulation. A larger value of R for the univariate or bivariate method results only in a marginal improvement of the failure probability estimate. Therefore, the value of R can be selected same as that of S. The univariate method ($S=R=1$) is the most computationally inexpensive method, but it is also the least accurate among the three decomposition methods. The bivariate ($S=R=2$) and trivariate ($S=R=3$) methods are highly accurate, but their computational efforts, particularly the effort of the trivariate method, are much larger than that of the univariate method.

DOI: 10.1002/nme

Table V. Component and system failure probabilities of a 10-bar truss.

Failure probability and effort	Univariate			Bivariate		Trivariate	
	$R=1$	$R=2$	$R=3$	$R=2$	$R=3$	$R=3$	Monte Carlo
$P^{*}_{F,1}$	1.04×10^{-4}	1.1×10^{-4}	1.1×10^{-4}	1.87×10^{-4}	1.86×10^{-4}	1.82×10^{-4}	1.82×10^{-4}
$P^{\dagger}_{F,2}$	2.75×10^{-4}	2.81×10^{-4}	2.81×10^{-4}	3.71×10^{-4}	3.7×10^{-4}	3.72×10^{-4}	3.72×10^{-4}
$P^{\ddagger}_{F,3}$	3.47×10^{-4}	3.59×10^{-4}	3.59×10^{-4}	5.12×10^{-4}	5.1×10^{-4}	5.1×10^{-4}	5.08×10^{-4}
No. of finite element analyses	41	761	8441	761	8441	8441	10^6

$^{*}P_{F,1}=P[1.7-v_3(\mathbf{X})<0]$.

$^{\dagger}P_{F,2}=P[10\,800-\sigma_1(\mathbf{X})<0]$.

$^{\ddagger}P_{F,3}=P[\{1.7-v_3(\mathbf{X})<0\}\cup\{10\,800-\sigma_1(\mathbf{X})<0\}]$.

5.5. *Example 5: probabilistic fracture mechanics*

The final example involves a circumferential, through-wall-cracked (TWC), non-linearly elastic cylinder that is subjected to a four-point bending, as shown in Figure 7(a). The cylinder has a mid-thickness radius $R_m=50.8\,\text{mm}$, a wall thickness $t=5.08\,\text{mm}$, and a symmetrically centered through-wall crack with the normalized crack angle $\theta/\pi=\frac{1}{8}$. The outer span $L_\text{o}=1.5\,\text{m}$ and the inner span $L_\text{i}=0.6\,\text{m}$. The cross-sectional geometry at the cracked section is shown in Figure 7(b). The cylinder is composed of an ASTM Type 304 stainless steel, which follows the Ramberg–Osgood constitutive equation [23]

$$\varepsilon_{ij}=\frac{1+v}{E}S_{ij}+\frac{1-2v}{3E}\sigma_{kk}\delta_{ij}+\frac{3}{2E}\alpha_0\left(\frac{\sigma_e}{\sigma_0}\right)^{m_0-1}S_{ij} \tag{40}$$

where σ_{ij} and ε_{ij} are stress and strain components, respectively, E is Young's modulus, v is the Poisson ratio, σ_0 is a reference stress, α_0 is a dimensionless material coefficient, m_0 is a strain hardening exponent, δ_{ij} is the Kronecker delta, $S_{ij}:=\sigma_{ij}-\sigma_{kk}\delta_{ij}/3$ is a deviatoric stress, and $\sigma_e:=\sqrt{3S_{ij}S_{ij}/2}$ is the von Mises equivalent stress. Table VI lists the means, standard deviations, and probability distributions of tensile parameters (E,α_0,m_0), four-point bending load (F), and fracture toughness (J_{Ic}). All random variables are statistically independent. In addition, $\sigma_0=154.78\,\text{MPa}$ and $v=0.3$. A finite element mesh of the quarter-cylinder model, consisting of 236 elements and 1805 nodes, is shown in Figure 7(c). Twenty-noded isoparametric solid elements from the ABAQUS library [24] were used, with focused singular elements at the crack tip. This type of TWC cylinders is frequently analyzed for fracture evaluation of pressure boundary integrity in the nuclear industry.

For a non-linearly elastic cracked solid, the J-integral is a useful crack-driving force that uniquely characterizes the asymptotic crack-tip stress and strain fields [23]. Therefore, a fracture criterion, where the J-integral exceeds the fracture toughness of the material, can be used to calculate the probability of fracture initiation: $P[J(\mathbf{X})>J_{Ic}(\mathbf{X})]$, in which the thickness-averaged J depends only on the first four random variables of $\mathbf{X}$ defined in Table VI. For the dimension-reduction

DOI: 10.1002/nme

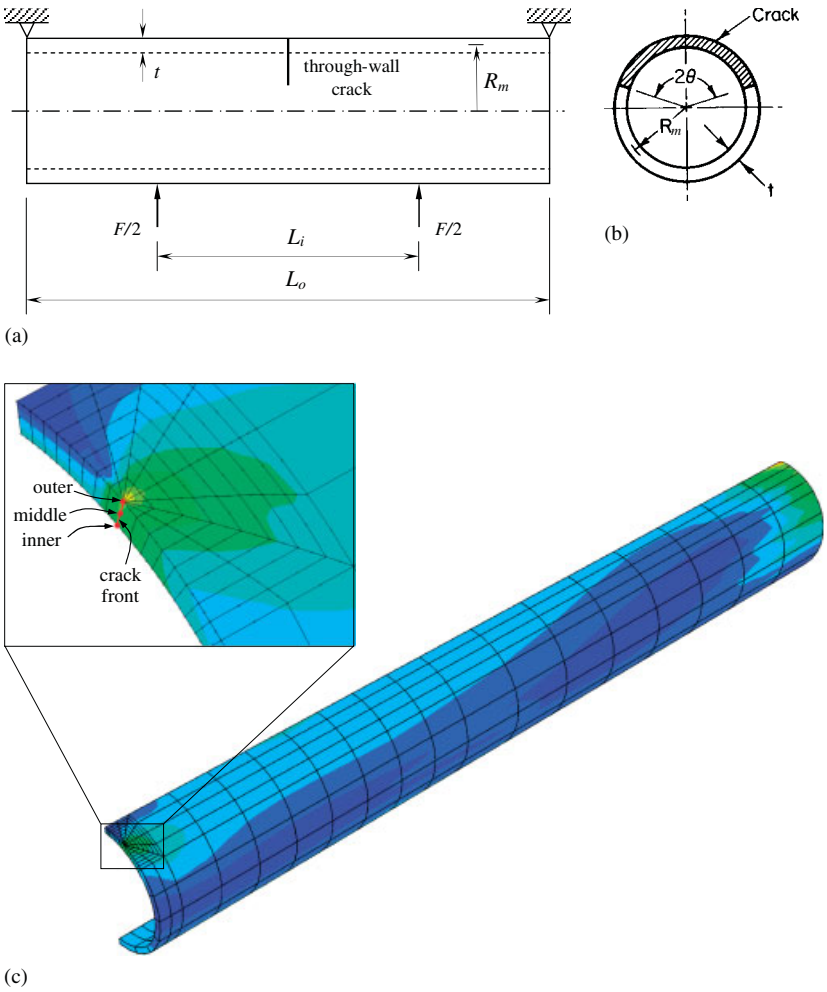

Figure 7. A through-wall-cracked cylinder under four-point bending: (a) geometry and loads; (b) cracked cross section; and (c) finite element discretization.

integration, the values of R and S are identical. The bivariate ($S=R=2$) decomposition method, using $m=4$, $n=5$, and only 113 ABAQUS-aided finite element analyses, predicts a fracture-initiation probability of 6.04×10^{-4}. The estimate of the fracture-initiation probability by the trivariate ($S=R=3$) decomposition method, which requires 369 finite element analyses, is 6.44×10^{-4}. Both estimates are similar and reasonably close to 5.91×10^{-4}, a value obtained from using the original bivariate decomposition method with sample points [5]. Due to expensive, non-linear, finite element analysis, direct Monte Carlo simulation was not feasible to verify the low probability in this example. Nonetheless, both Examples 4 and 5 demonstrate the non-intrusive nature of the proposed decomposition method, which can be easily integrated with external numerical analysis codes for solving complex stochastic problems.

DOI: 10.1002/nme

Table VI. Statistical properties of random input for a through-wall-cracked cylinder.

Random variable	Mean	Standard deviation	Probability distribution
Elastic modulus, E (GPa)	182.7	18.27	Gaussian
Ramberg–Osgood coefficient, α_0	8.073	3.544	Lognormal
Ramberg–Osgood exponent, m_0	3.8	0.5548	Lognormal
Four-point bending load, F (kN)	28	2.8	Gaussian
Initiation toughness, J_{Ic} (kJ/m^2)	1242.6	584.02	Lognormal

6. CONCLUSIONS AND OUTLOOK

A new polynomial dimensional decomposition method was developed for solving stochastic problems commonly encountered in engineering disciplines and applied sciences. The method is based on a hierarchical decomposition of a multivariate response function in terms of variables with increasing dimensions. Compared with the previous development, the new decomposition method does not require sample points around the mean input to approximate the component functions. Instead, orthogonal polynomial basis functions in the Hilbert space, ranging from the Hermite, Legendre, and Jacobi polynomials, were employed, yielding the Fourier-polynomial expansion of the component functions. An innovative dimension-reduction integration scheme was applied for efficiently calculating the expansion coefficients. The end result is a convergent sequence of lower-variate estimates of the probabilistic characteristics of a generic stochastic response. The method is non-intrusive in the sense that the expansion coefficients are obtained by calculating responses at selected deterministic input defined by the integration points. Therefore, the method can be easily adapted to solving complex stochastic problems requiring external commercial codes.

The decomposition method was employed to solve five examples, where the performance functions are polynomials or non-polynomials, include mixtures of Gaussian and non-Gaussian random variables, and are described by simple mathematical functions or mechanical responses from linear or non-linear finite element analysis. The results indicate that the decomposition method developed, in particular the bivariate and trivariate versions, provides very accurate estimates of the tail distribution of random response or reliability. The computational effort by the univariate method varies linearly with respect to the number of random variables or the number of integration points. Therefore, the univariate method is economic. In contrast, the bivariate or trivariate method, which generally outperforms the univariate method, demands a quadratic or cubic cost scaling, making either method also more expensive than the univariate method. Nonetheless, all three versions of the decomposition method are far less expensive than the direct Monte Carlo simulation.

There are important differences between the dimensional decomposition and polynomial chaos expansion methods. The dimensional decomposition is a finite sum, whereas the polynomial chaos expansion is an infinite series and contains an infinite number of random variables. More importantly, the dimensional decomposition is structured with respect to the degree of cooperativity between a finite number of random variables. Consequently, if a response is highly non-linear but contains rapidly diminishing cooperative effects of multiple random variables, the dimensional decomposition is highly effective. Nonetheless, the polynomial dimensional decomposition and polynomial chaos expansion methods are both convergent, but in the mean square sense. Further work is necessary to examine the convergence modes and properties of these methods when a

DOI: 10.1002/nme

stochastic response is discontinuous, non-smooth, or a function of mixed random variables with an arbitrary probability measure.

ACKNOWLEDGEMENTS

The author would like to acknowledge the financial support from the U.S. National Science Foundation under Grant numbers DMI-0355487 and CMMI-0653279.

REFERENCES

1. Grigoriu M. *Stochastic Calculus—Applications in Science and Engineering*. Birkhäuser, Springer: New York, NY, 2002.
2. Schueller GI. IASSAR Subcommittee on Computational Stochastic Structural Mechanics. 'A state-of-the-art report on computational stochastic mechanics'. *Probabilistic Engineering Mechanics* 1997; **12**(4):197–321.
3. Bellman R. *Dynamic Programming*. Princeton University Press: Princeton, NJ, 1957.
4. Xu H, Rahman S. A generalized dimension-reduction method for multi-dimensional integration in stochastic mechanics. *International Journal for Numerical Methods in Engineering* 2004; **61**:1992–2019.
5. Xu H, Rahman S. Decomposition methods for structural reliability analysis. *Probabilistic Engineering Mechanics* 2005; **20**:239–250.
6. Caflisch RE, Morokoff W, Owen AB. Valuation of mortgage backed securities using Brownian bridges to reduce effective dimension. *Journal of Computational Finance* 1997; **1**:27–46.
7. Hoeffding W. A class of statistics with asymptotically normal distributions. *Annals of Mathematical Statistics* 1948; **19**:293–325.
8. Efron B, Stein C. The jackknife estimate of variance. *Annals of Statistics* 1981; **9**:586–596.
9. Sobol IM. Theorems and examples on high dimensional model representations. *Reliability Engineering and System Safety* 2003; **79**:187–193.
10. Rabitz H, Alis O. General foundations of high dimensional model representations. *Journal of Mathematical Chemistry* 1999; **25**:197–233.
11. Li G, Wang SW, Rabitz H. Practical approaches to construct RS-HDMR component functions. *Journal of Physical Chemistry A* 2002; **106**:8721–8733.
12. Abramowitz M, Stegun IA. *Handbook of Mathematical Functions* (9th edn). Dover Publications: New York, NY, 1972.
13. Boyd JP. *Chebyshev and Fourier Spectral Methods*. Dover Publications: New York, NY, 2000.
14. Wiener N. The homogeneous chaos. *American Journal of Mathematics* 1938; **60**(4):897–936.
15. Ghanem RG, Spanos PD. *Stochastic Finite Elements*: *A Spectral Approach*. Springer: New York, NY, 1991.
16. Choi SK, Grandhi RV, Canfield RA, Petit CL. Polynomial chaos expansion with latin hypercube sampling for estimating response variability. *AIAA Journal* 2004; **42**:1191–1198.
17. Tatang MA, Pan W, Prinn RG, McRae GJ. An efficient method for parametric uncertainty analysis of numerical geophysical models. *Journal of Geophysical Research* 1997; **102**:21925–21932.
18. Rahman S, Xu H. A univariate dimension-reduction method for multi-dimensional integration in stochastic mechanics. *Probabilistic Engineering Mechanics* 2004; **19**:393–408.
19. Xiu D, Karniadakis GE. The Wiener–Askey polynomial chaos for stochastic differential equations. *SIAM Journal on Scientific Computing* 2003; **187**:137–167.
20. Melchers RE, Ahammed M. A fast approximate method for parameter sensitivity estimation in Monte Carlo structural reliability. *Computers and Structures* 2004; **82**(1):55–61.
21. Hong HP, Lind NC. Approximate reliability analysis using normal polynomial and simulation results. *Structural Safety* 1996; **18**(4):329–339.
22. Penmetsa R, Grandhi R. Adaptation of fast Fourier transformations to estimate structural failure probability. *Finite Elements in Analysis and Design* 2003; **39**:473–485.
23. Anderson TL. *Fracture Mechanics*: *Fundamentals and Applications* (3rd edn). CRC Press: Boca Raton, FL, 2005.
24. ABAQUS. *User's Guide and Theoretical Manual*, Version 6.6. ABAQUS Inc.: Providence, RI, 2006.

DOI: 10.1002/nme